Bibliography

SLAC Studies

G.A.Loew and J.W.Wang, SLAC-PUB-4647, 1988.

G.A.Loew and J.W.Wang, SLAC-PUB-5320, 1990.

I. Ben-Yaacov, C.H. Back, and R.E. Kirby, SLAC-PUB-7265, 1996.

Geneva Group

Ph.Niedermann, N.Sankarraman, R.J.Noer, and O.Fischer, J. Appl. Phys. 59,892,1986.

R.J.Noer, Ph.Niedermann, N.Sankarraman, and O.Fischer, J. Appl. Phys. 59,3851,1986.

Saclay Group

M.Jimenez, R.J.Noer, G.Jouve, C.Antoine, J.Jodet, and B.Bonin, J. Phys. D Appl. Phys. 26, 1503, 1993.

M.Jimenez, R.J.Noer, G.Jouve, J.Jodet, and B.Bonin, J. Phys. D: Appl. Phys. 27,1038,1994.

Wuppertal Group

E.Mahner, N.Minatti, H.Piel, and N. Pupeter, Applied Surface Science, **67, 23, 1993.**

N.Pupeter, T.Habermann, A.Kirschner, E.Mahner, G.Müller, H. Piel, Applied Surface Science, **94/95, 94, 1996.**

Cornel1Group

J.H.Graber, **SRF930208-03,** Thesis Chapter, **1993.**

J.Knobloch, R.Durand, H.Muller, and H.Padamsee, SRF950427-07, 1995 PAC, Dallas, **1995.**

H. Padamsee, RF96, 1996.

J.Knobloch and H.Padamsee, Particle Accelerators, 53, **53,1996.**

Aston Group

K.H.Bayliss and R.V.Latham, Vacuum, **35,211,1985.**

R.V.Latham, K.H.Bayliss, and B.M.Cox, J.Phys.D: Appl.Phys. **19,219,1986.**

N.S.Xu and R.V.Latham, J.Phys.D: Appl.Phys. **19, 477, 1986.**

R.V.Latham and N.S.Xu, Vacuum, **42,1173,1991.**

N.S.Xu and R.V.Latham, J.Phys.D: Appl.Phys. 27, 2547, 1994.

Miscellaneous

R.H.Fowler and L.Nordheim, Proc.Royal Soc. London **119A, 173, 1928.**

H.Matsumoto, M.Akemoto, H.Hayano, A.Miura, T.Naito, and S.Takeda, KEK Preprint **9147, 1991.**

W.Peter, E.Garate, J.Shiloh, F.Mako, and R.Silberglitt, FM Technologies, APS Meeting Poster, Denver, **1996.**

Basic Picture from Literature

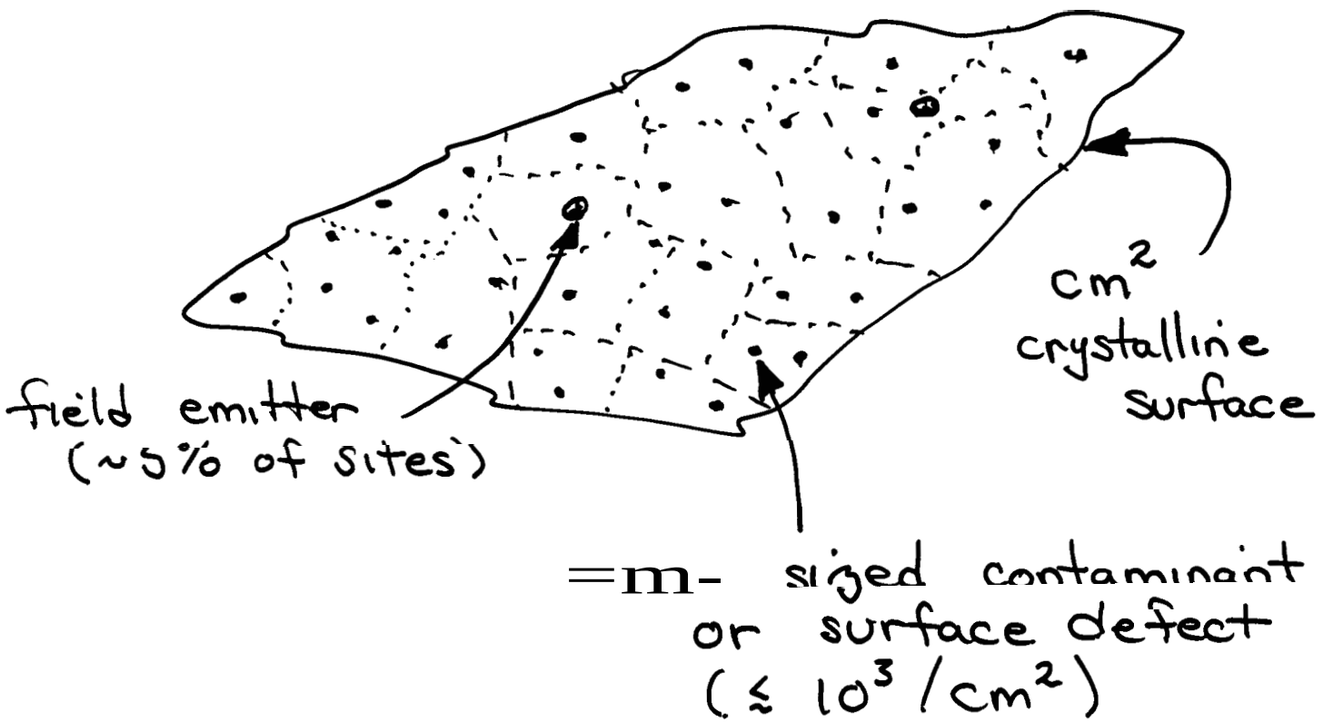

Emitters are rare and predominantly (likely always) contaminants or surface defects introduced during manufacture and handling.

Padamsee
RF96

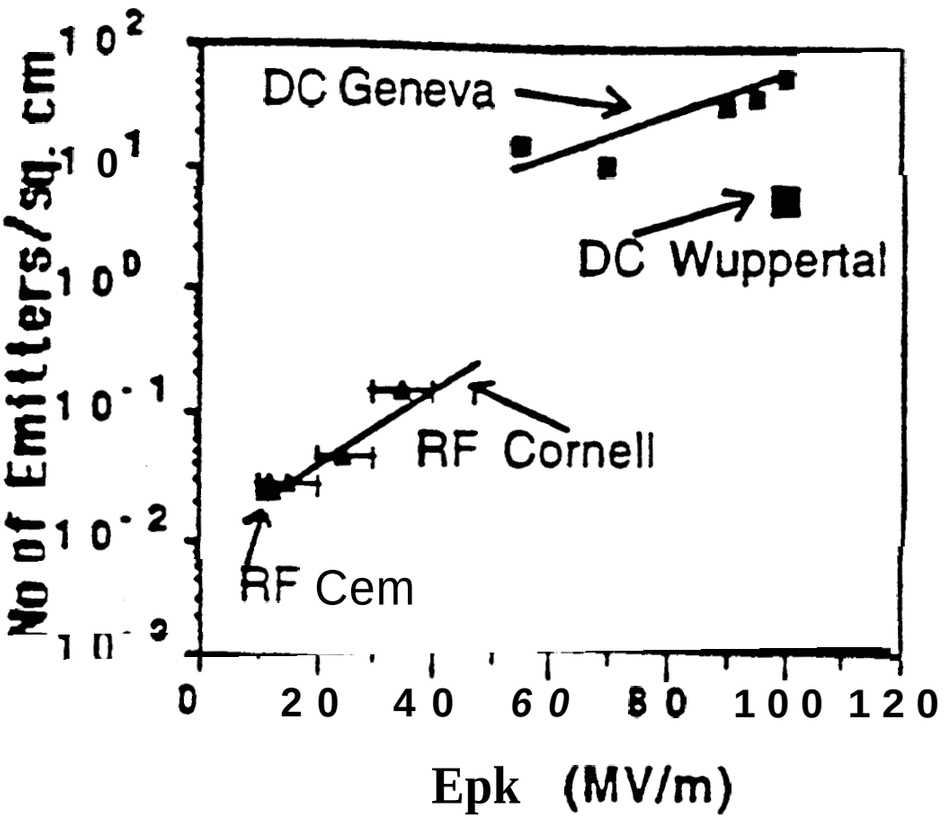

Consider (e.g. DC HV Studies)

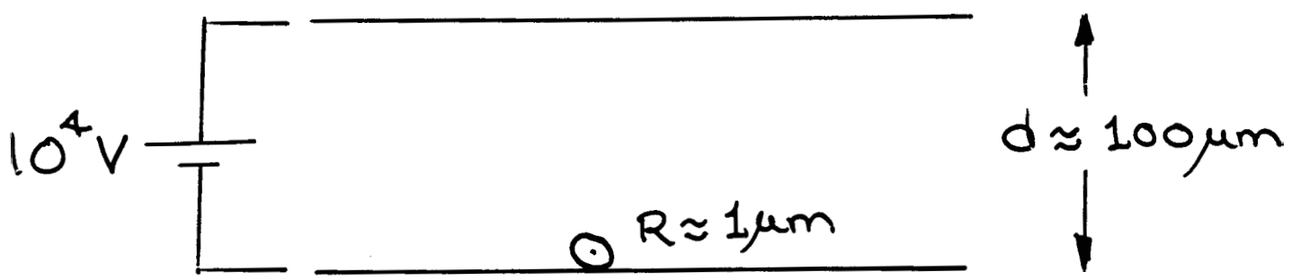

$$E = 10^4 V / 10^{-4} m = 100\ MV/m$$

Now $\phi_{sphere} \approx Q/R \equiv 10^4 V$

and, $E_{sphere} \approx Q/R^2 = 10^4 V / 10^{-6} m = 10 GV/m$

which is ~ Fowler-Nordheim limit for emission (4 eV work function).

→ micron-sized contaminants on surfaces at 100 MV/m will emit.

Geneva Group **1986**

See slides of apparatus.

Features:

1. In-situ SEM and Auger; spatial resolution 0.5 μm.
   - Previously slits of several microns.

2. In-situ field emission electron detectors
   - Previous use of X-rays
   - Good sensitivity to all Z.

3. Unbiased broad survey:
   - 1 mm diameter anode tips - survey scans
   - Few micron diameter tips - microscans
   - Survey cm^2 area cathodes.

4. "Constant current" (voltage feedback)
   - Max current of 1nA
     or max 100 MV/m.
   - Good dynamic range - Keithley pA meter.

5. "Load-lock" preparation chamber for UHV control.

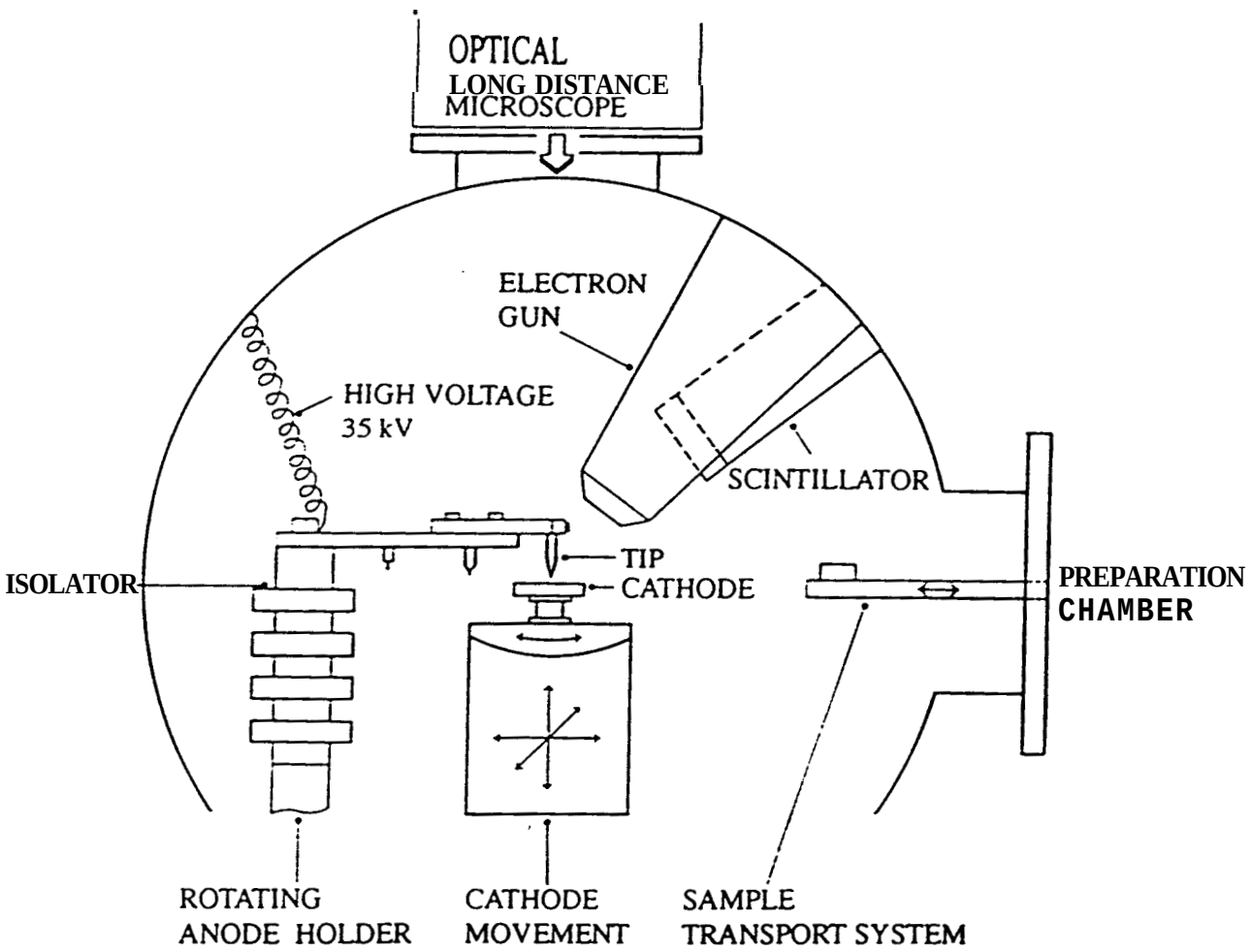

SEM and the field emission scanning microscope used for the FE experiments inside the UHV analysis chamber.

ent is an optical pyrometer we have carried out HT's only above 800 °C.

For the field emission scanning measurements, a manipulator (Fig. 2) was specially designed. x, y, and z motions with ranges of 25 mm for x and y and 12 mm for z are performed by linear tables inside the vacuum. These consist of austenitic stainless steel guiding surfaces[11] and martensitic

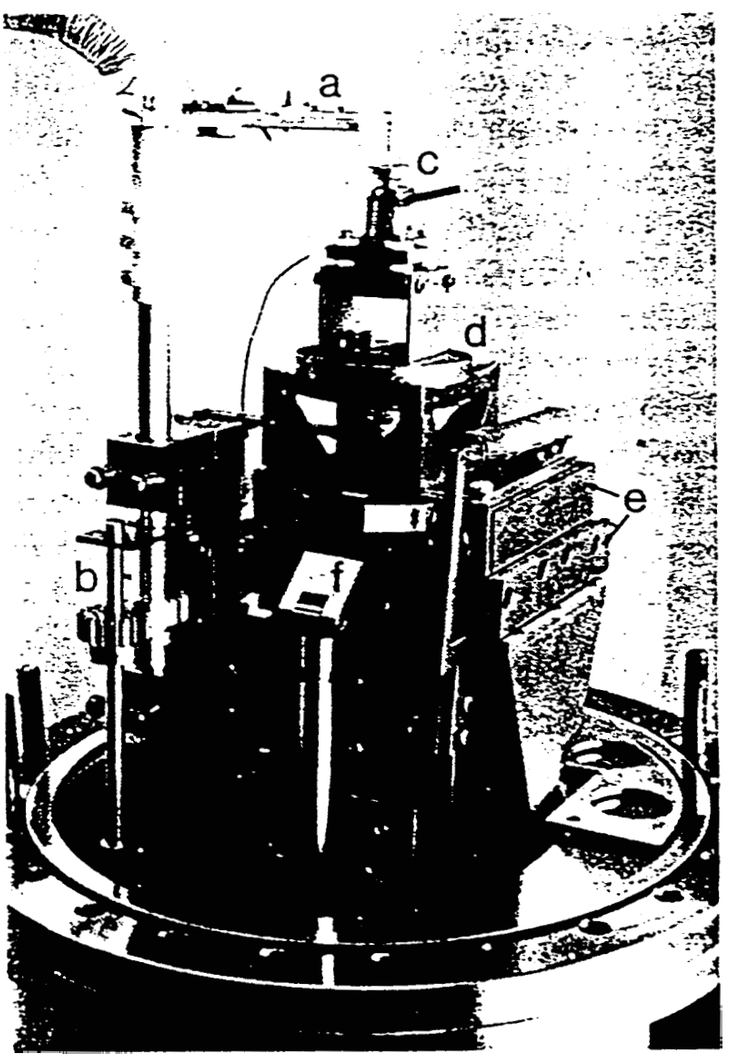

FIG. 2. The sample manipulator used for the FE experiments. On top, the anode holder (a) with its rotation mechanism (b) on the left. Below the sample (c) are the tilt mechanism (d) and the x- andy-linear tables (e). In the front, the lever (f) for the x motion is seen. The z linear table is not visible. Below the mounting flange, a bellows (not seen) allows the adjustment of the entire mechanical unit.

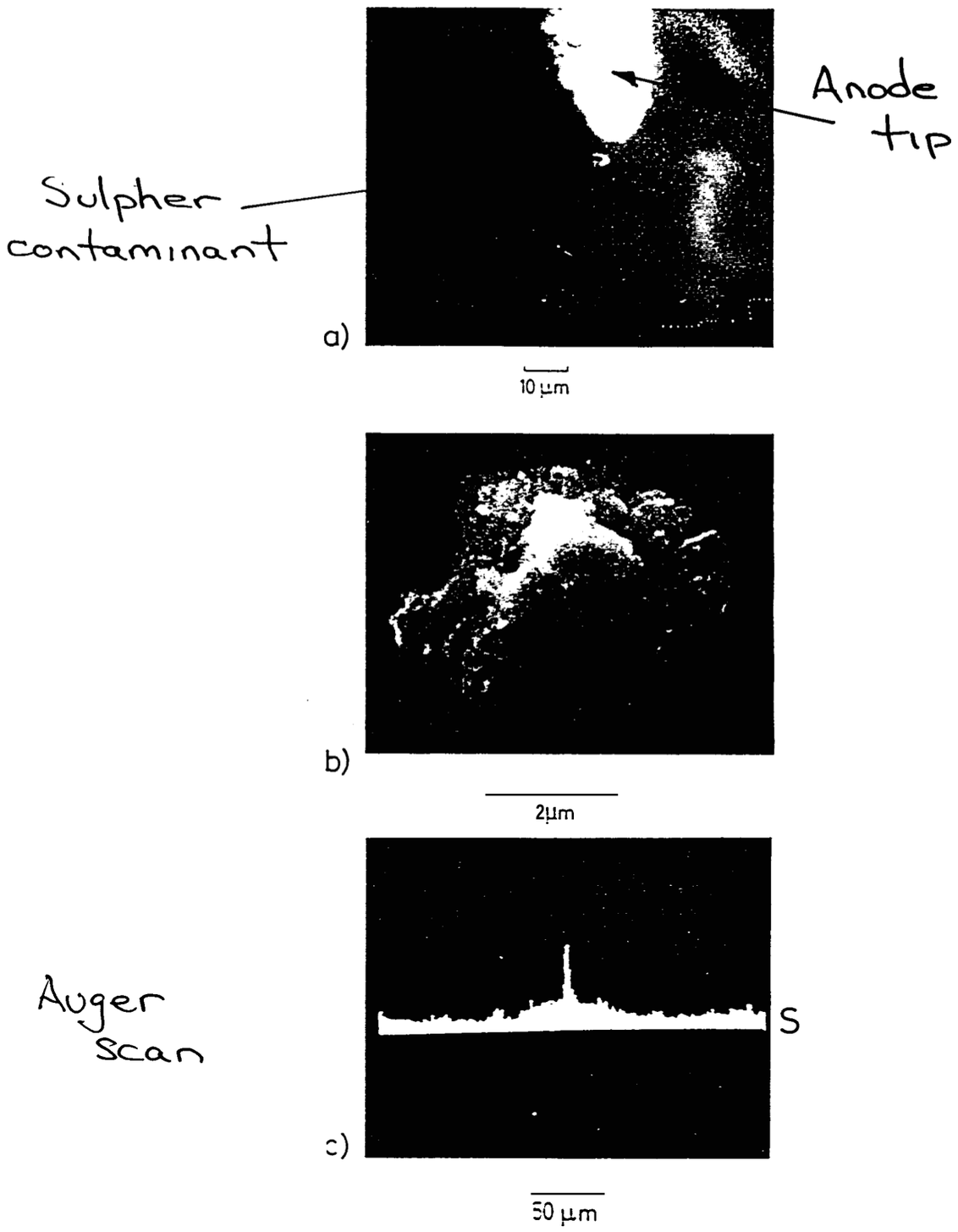

FIG. 9. Sulfur FE site. (a) SEM image. showing rhe point anode at 10 μm above the sire. (b) SEM image of the same sire taken in a high resolution SEM. (c) Auger line scan across the particle (before sputtering) showing he S peak-to-peak height.

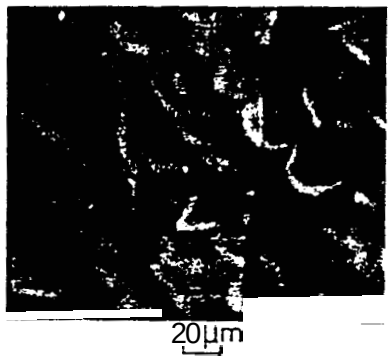

Initial contact area

Carbon (Auger)

b)

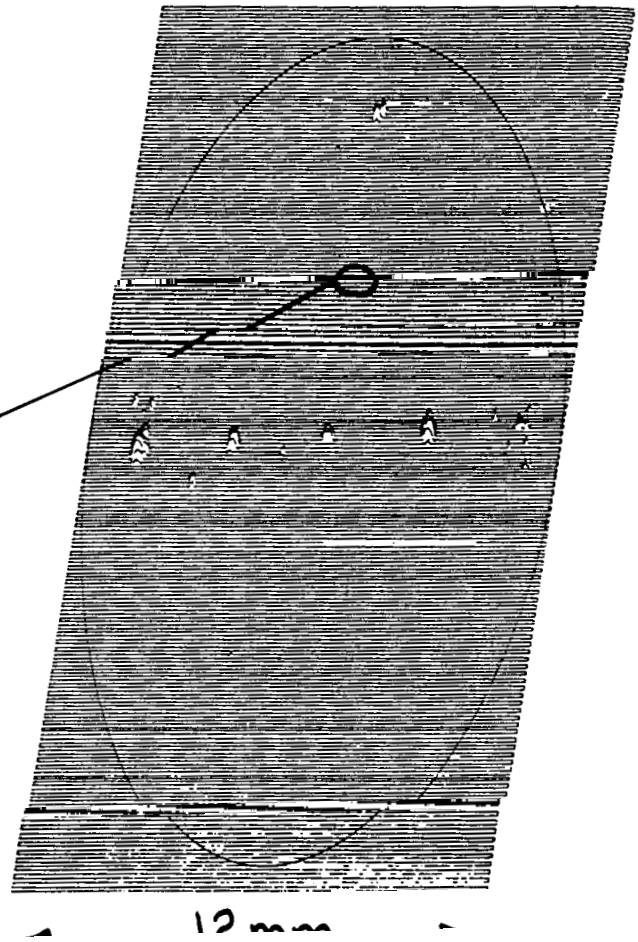

FIG. 1. (a) SEM photograph of carbon deposit C7, *on* pure Nb cathode. (b) Same with Auger *carbon* map superposed. Dashed h e shows approximate region of contact between carbon point and Nb surface

Broad area scan showing 9 sites with carbon deposrts.

Emitting microsites

FIG. 5. Same as Fig. 1(a) with positions of emission sites indicated. (Numbers correspond to those on Fig. 4.)

Precision scan of site 7.

Observations (Geneva):

1. Nb surfaces of cm2 can be prepared with no emitters (with heat treatment).

2. Field emission occurs at localized sites with dimensions typically ≤ micron. Most (at least 80%) are due to contaminants:

Ag, C, Ca, Cu, S, Si, Mn

and most are found to be conducting (SEM).

3. Potential emitters are sparse objects on the surface, and only a fraction (5-10%) of the particles found on the surface are actually emitters.

4. Emitters do not preferentially occur at grain boundaries and oxidation of the Nb surface (even ~ 130nm anodize) does not alter results (after "switch-on").

5. Brief exposures (1-2 hrs) to ambient atmosphere do not alter results.

6. Artificially created carbon, sulpher, and MoS2 sites behave like naturally occuring ones.

Saclay Group 1993-1994

- Similar techniques - broad and microtip scans of electro-polished Nb and mechanically polished (alumina slurry) Au cathodes.

- Artificial ensemination of cathodes with various contaminants:

Ag, Au, Al_2O_3, Nb, Ni, SiO_2, Ti

of 5-25 micron dimensions.

- Deliberate damage sites created on surfaces.

Features:

1. In-situ SEM and EDX analyses.

2. Threshold currents of several pA (Keithley) and total current limited to 100pA.

(a)

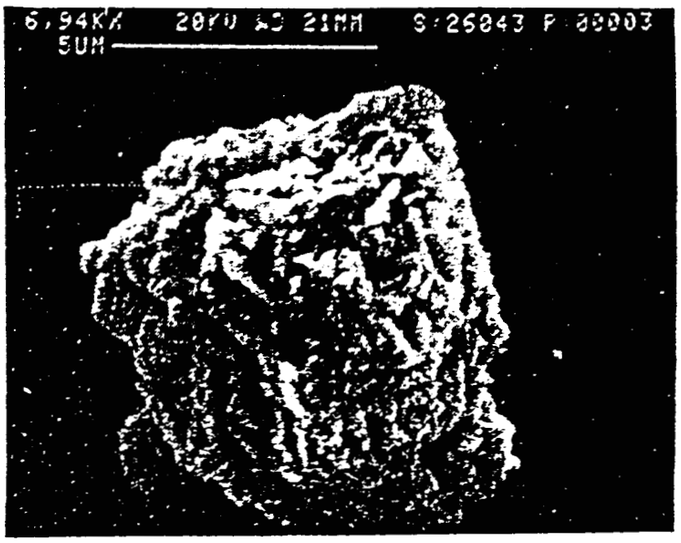

(b)

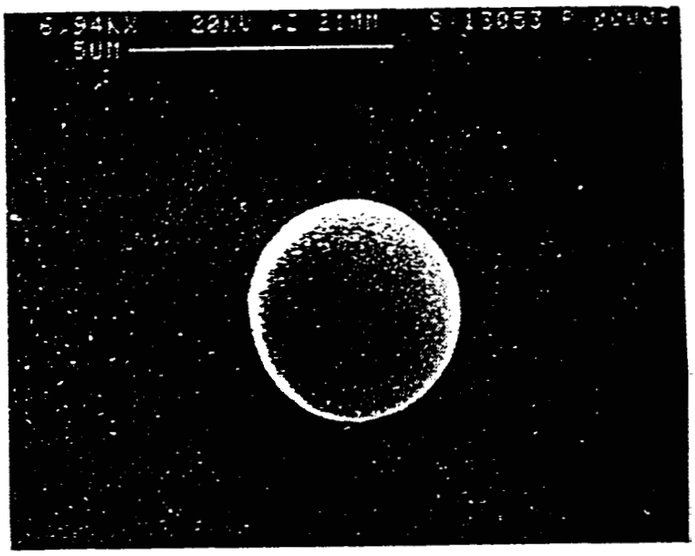

Figure 1. Nickel particles used as potential emission sites: *(a)* irregular, ***(b)*** spherical.

Ni on Nb

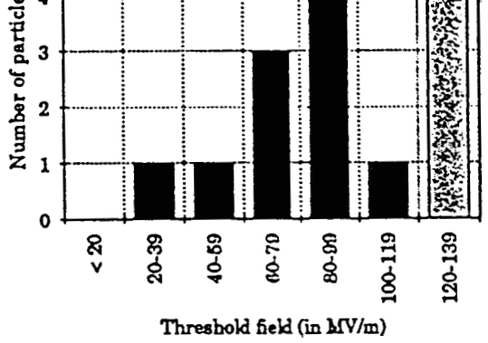

"Natural"

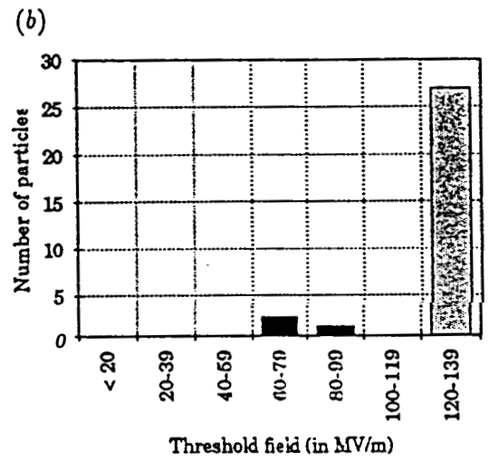

Figure **2.** Emission tests for Ni particles on a Nb substrate. Dark bars show threshold fields for measured emission; light bars show the maximum field attained when no emission was seen: ***(a)***irregular particles, ***(b)***spherical particles.

Fe on Nb

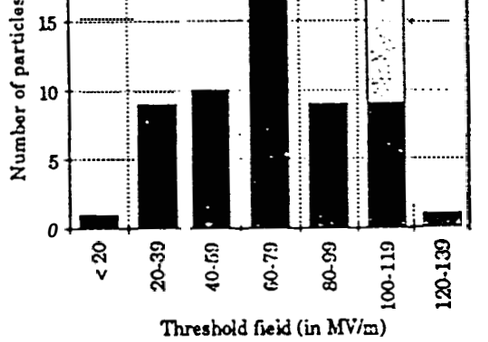

"Spherical"

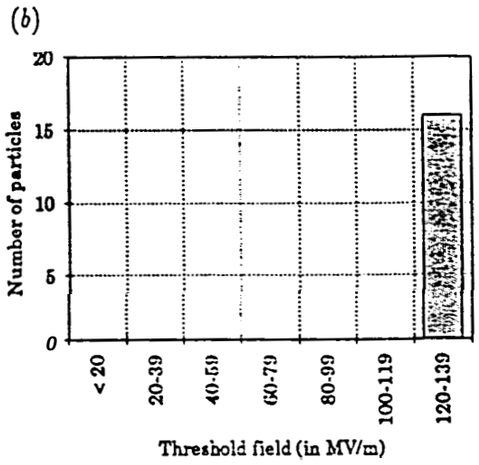

Figure 3. Emission tests for Fe particles on a Nb substrate. Dark bars show threshold fields for measured emission; light bars show maximum field attained when n emission was seen: ***(a)***irregular particles, (6) spherical particles.

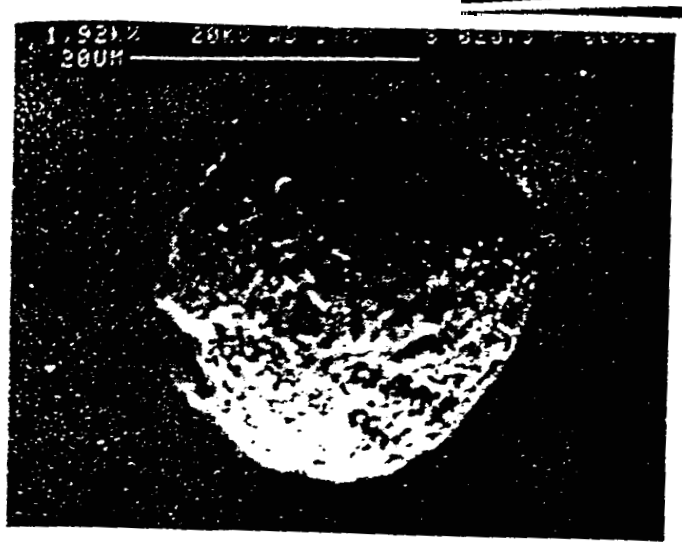

Figure 5. 'Point' mechanical damage site.

(*a*)

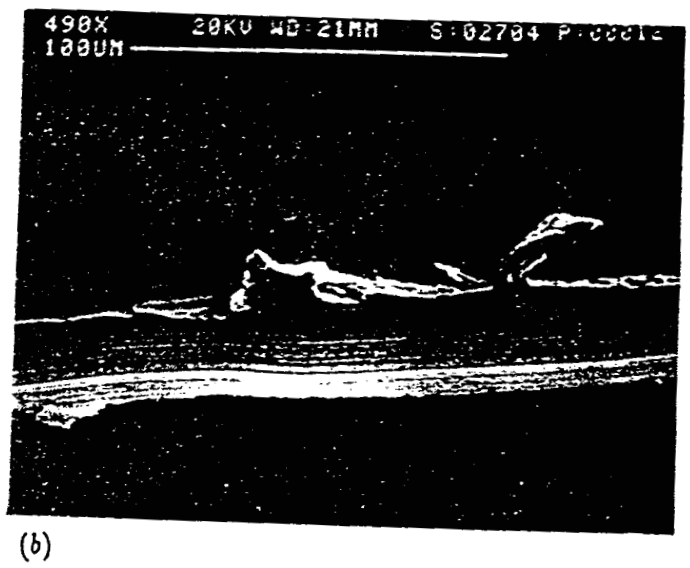

(*b*)

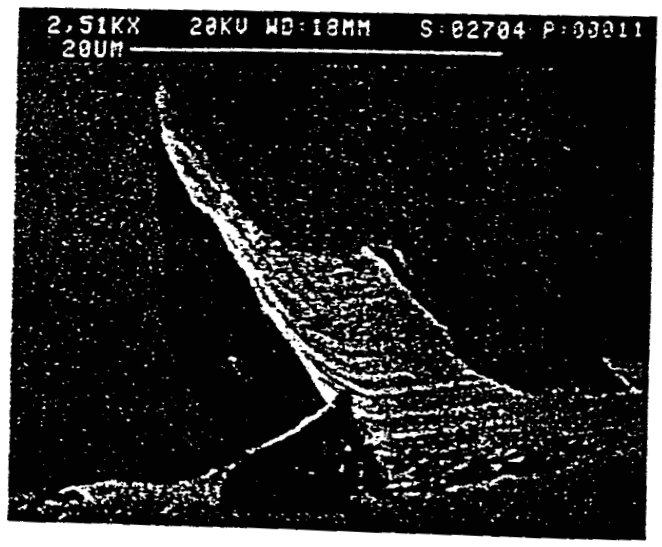

Figure 6. 'Scratch' mechanical damage site: (*a*) upper view, (*b*) lateral view.

Properties of Damage Sites

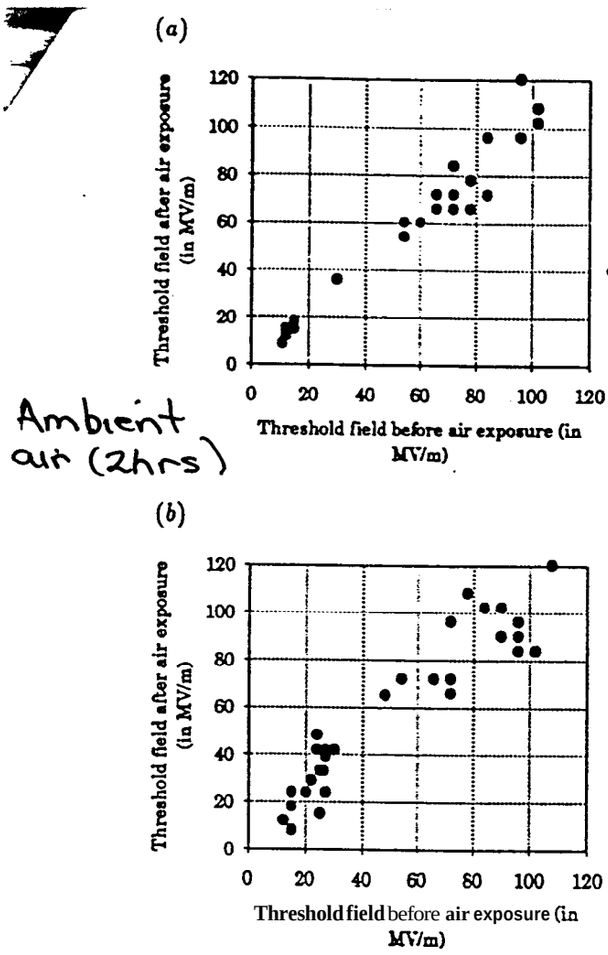

Figure 8. Effect of an air exposure on the threshold fields of point defects on a Au substrate *(a)* ana on a Nb substrate *(b)*.

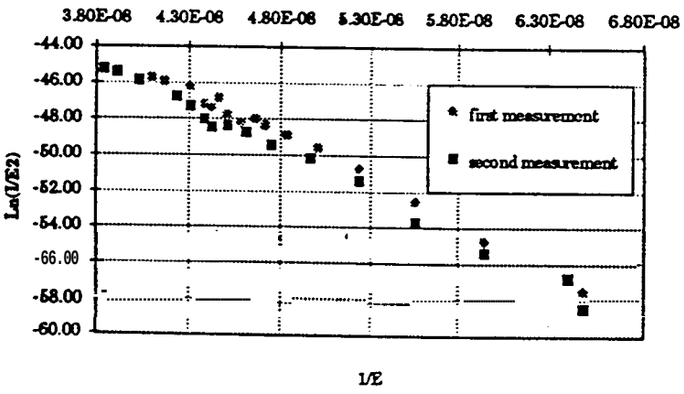

Figure 9. A Fowler–Nordheim plot of the emission

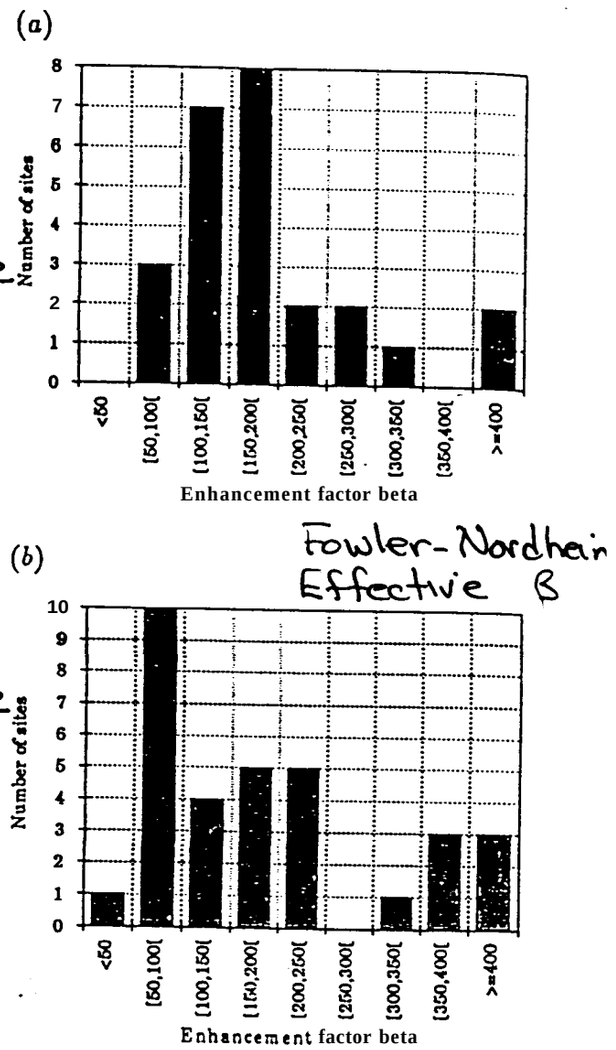

Figure 10. .Enhancement factor β extracted from our current versus field values for mechanical damage sites on a Au substrate *(a)* and on a Nb substrate *(b)*.

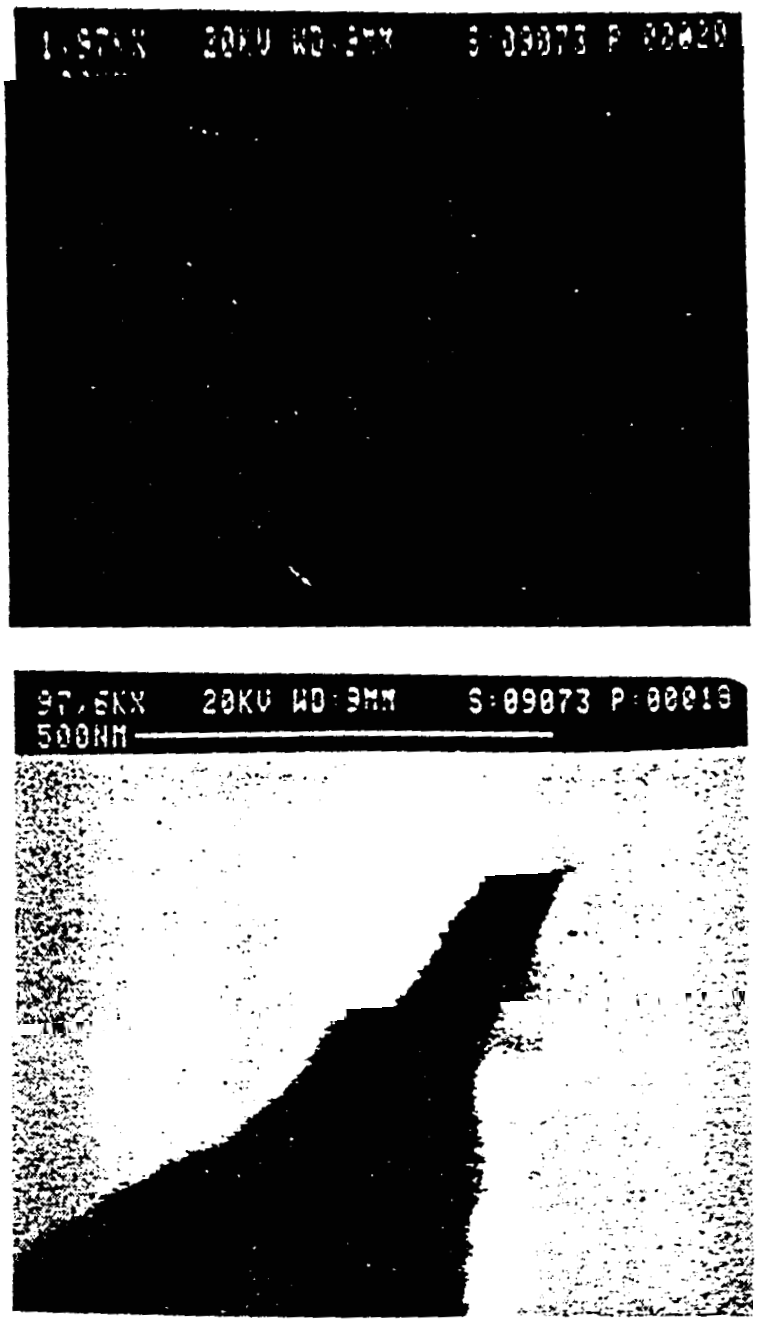

Figure 13. Geometrical defect with two superposed projections (threshold field 15 MV m^{-1}).

Ex-situ high resolution SEM.

Tips-on-Tips do exist.

Observations (Saclay):

1. Attempts to sprinkle particles on clean, dry cathode met with failure; application of even a low field resulted in disappearance of the particles.

2. Had to use liquid nitrogen to afix contaminants. This is similar to experiences of earlier workers - *e.g.* carbon studies on Nb by the Geneva group.

3. Insulators (Al_2O_3 and SiO_2) are not strong emitters up to peak gradients (100MV/m).

4. Emission from conductors depends on history of application of voltage.

- "Switch on" effect.
- Emitters always in contact with substrate

after switch on (even with Nb anodizing).

5. Perfectly round spheres never emit whereas naturally occuring contaminants do.

6. Exposure to ambient air (2 hrs) had little effect.

7. Easy to replicate threshold fields, and Fowler-Nordheim plots and parameters with artificial contaminants and intentional damage of cathode surfaces.

Wuppertal Group - 1996

- Repeat of earlier Geneva work, but extended to Cu and Al.

- Similar techniques:

  In-situ SEM and optical microscope.
  Broad and microtip surface scans.
  Constant current with 1-40nA limits.
  Ex-situ high-resolution SEM; 100nm resolution.

- Cathode preparations:

  Mechanically **polished** (diamond) Cu, Nb, and Al.
  8nm on copper (both OFHC and SE)
  10nm on niobium
  55nm on aluminum
  Ultra-pure (not clear if high-pressure) water rinse.
  Nitrogen gas dry and clean room handling through-out.

the literature [10–13] proves that the mechanical polishing and final ultra-pure water rinsing of copper cathodes results in a very strong reduction of EFE.

On chemically polished copper cathodes an additional class of emitters was observed, which explains the rising emitter density compared with the mechanically polished ones, see Fig. 1. Etched defects in the rough copper surfaces (Fig. 5) tend to emit above 100 MV/m. At most of the investigated etch defects, sulphur as a foreign element contamination was detected. Since the chemical polishing does not contain sulphur, we assume that the etched defects originated from the chemical polishing of sulphur clusters in the copper. Therefore, the similarity of emission behaviour of SE and OFHC copper after chemical polishing can possibly be explained by the content of S (~ 5 ppm) which is equal for both kinds of copper. Other experiments also showed the stimulation of EFE by sulphur segregation or MoS_2 particles [2].

4.3. Aluminium cathodes

On *mechanically polished* Al cathodes, most emission sites did not appear until 100 MV/m. Two-thirds of the emitters were localised as surface defects combined with an enhanced concentration of Si, Mg, Fe and Mn, which are the main foreign elements of AlMgSil. The distribution of these elements was very inhomogeneous and, by means of EDX, an enhancement at the bright dots by a factor

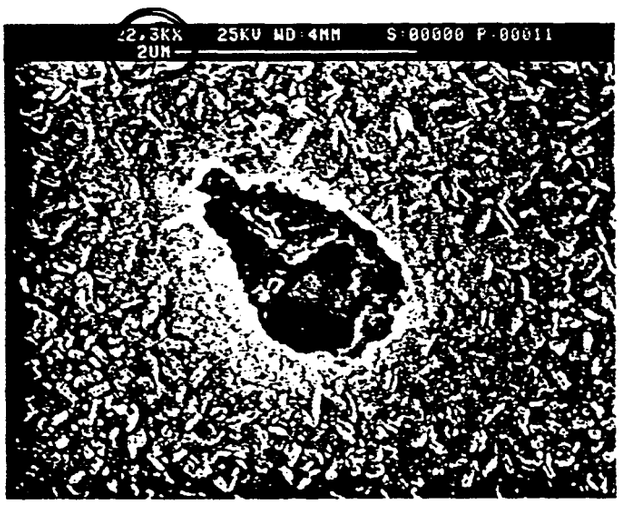

Fig. 5. SEM image of an S contaminated etched defect on chemically polished Cu ($E_{on} = 142$ MV/m, $\beta = 26$, $S = 6 \times 10^{-11}$ cm^2).

Note scale

Fig. 6. SEM *image* of a surface defect on mechanically polished Al with strongly enhanced concentration of Si, Mg, Fe and Mn in the brighter area (arrow) (E, = 58 MV/m, $\beta = 62$, $S = 3.9 \times 10^{-12}$ cm^2).

of 5–6 compared with the hole surface was detected. Possibly, an enhanced stiffness of the foreign inclusions caused surface damage during mechanical polishing, which was observed at these bright dots. A typical example of such an emitting inclusion is shown in Fig. 6.

After high field measurements, one-third of the localised sites were identified as emitting craters similar to those on Nb and Cu. Probably, the prebreakdown currents which resulted in the molten craters were also caused by damaged inclusions. Therefore, the use of Al for high field vacuum devices with very homogeneous elemental composition is needed to avoid EFE above 100 MV/m from inclusions. Nevertheless, similar emitter densities on Al, already at five times lower field strength as reported in the literature [14], demonstrate the improvement of the mechanical surface preparation technique described here.

4. Discussion

In our experiments, different kinds of emitting sites have been detected. To investigate whether or not the observed emitter types (categories I–V) show different emission behaviour as a function of the type of metal, the average values of E_{β}, β and S are listed in Table 1. On Nb, the surface defects after mechanical polishing (Ia) as well as macro-

Table 1
Average values of emission parameters E_{on}, β, and S of different emitter types are presented as a function of metal; an average work-function of 4 eV was assumed for the calculation of the Fowler–Nordheim parameters β and S of emission sites on Nb; for Cu and Al, values of 4.5 eV and 3.74 eV, respectively, were used

Emitter types in dependence on metal	E_{on} (MV/m)	β	S (cm^2)
(Ia) Defects on mechanically polished Nb	54	102	6×10^{-13}
(Ib) Scratches on chemically polished Nb	53	105	1×10^{-13}
(IIa) Particles on Nb	78	64	3×10^{-11}
(IIb) Particles on Cu	70	76	2×10^{-10}
(IIIa) Molten craters on Nb	108	37	3×10^{-10}
(IIIb) Molten craters on Cu and Al	99	42	5×10^{-10}
(IV) Etch pits on chemically polished Cu	112	24	3×10^{-7}
(V) Inclusions on mechanically polished Al	76	52	3×10^{-11}

scopic scratches with steel contamination (Ib) showed stronger β values but more than two orders of magnitude smaller S values in comparison with the other kinds of emitters. Within the category of particle emitters, no significant difference in FE behaviour was observed between Nb (IIa) and Cu (IIb). Moreover, the FE behaviour of molten emitting craters (IIIa, b) did not Seem to depend on the cathode material, despite the significantly lower melting points of Cu and Al compared with that of Nb.

At present, our experiments do not indicate that the EFE mechanism is influenced by the intrinsic properties of the metal or its oxides, because similar emitter types on Nb, Cu, and Al showed similar emission behaviour. Furthermore, we never observed intrinsic emission up to $E = 200$ MV/m, e.g. from grain boundaries. In contrast, foreign elements or particles were definitely found at the emission sites in many experiments. Therefore, the predicted electron emission of metal–insulator–vacuum (MIV) structures [15] that consist only of the bulk metal and its oxide can be ruled out for broad area cathodes. Proposals of geometrical field enhancement alone, provided by nm-sized microprotrusions [16], can not describe our results because of the wide range of measured S values. Alternatively, the foreign elements mostly detected at the emission sites could lower the local work-function, which would result in reduced β values and a systematic shift to higher S values of about 2–3 orders of magnitude. The detection of sometimes very unrealistic S values (e.g. 1×10^{-17} cm^2, $6\times10^{+15}$ cm^2) indicates that the EFE mechanism is of a much more complex nature. Moreover, for many emitters of each category an interesting "switch on" phenomenon was observed. After a first activation in a high electrical field, the emitters were already active at ~70% of that field. Our experiments support the emission model of metal–insulator–metal (MIM) structures [17]. In this model the "switch on effect" is explained by the formation of conduction channels in the insulating interface due to the high electrical fields.

5. Conclusions

Two improved preparation methods for metallic cathodes were presented. For the first time, lowest emitter densities between 0.6/cm^2 and 6/cm^2 at $E = 100$ MV/m were systematically achieved on chemically polished Nb and Cu, as well as on mechanically polished Cu and Al after final rinsing with ultra-pure water. Strongest reduction of EFE up to $E = 200$ MV/m was observed on the improved chemically polished Nb cathodes and mechanically polished Cu cathodes. Because only particle emitters were identified but no surface defects, the success of both preparations seems to be limited only by the quality of the final ultra-pure water rinsing, not by the polishing technique. No difference of field emission behaviour was observed between SE copper and OFHC copper. Further investigations on the improvement of mechanical polishing of niobium are in progress. By means of the described wet chemical etching for the preparation of niobium surfaces, higher electrical field strength than is usual today should be achieved in superconducting accelerating resonators. We showed that the described mechanical polishing followed by ultra-pure water rinsing is very useful for the suppression of EFE in Cu or Al high-voltage vacuum devices up to field strengths of 100 MV/m.

Five emitter types were classified by different morphology and emission behaviour to investigate the emission process itself: particles on Nb and Cu, surface defects on Nb, S contaminated etched defects on Cu, inclusions in Al and molten craters on all three metals. No dependence of emission behaviour on the intrinsic properties of all metals and their oxides were found within these emitter categories. Additionally, no intrinsic emission, without a surface anomaly, was observed up to $E = 200$ MV/m. At many emission sites foreign elements were detected that stimulate EFE. The wide range of determined S values ruled out a purely geometrically enhanced FE and the authors assume an EFE mechanism similar to that proposed in the MIM model, explaining the often observed "switch on" effect.

Acknowledgements

The authors wish to thank J. Engemann for providing the high resolution SEM. The sample preparation in the TTF cleanroom facility with A. Matheisen and the financial support from DESY are gratefully acknowledged.

Observations (Wuppertal):

1. All emission sites were either
   microparticles
   microscratches
   or etch pits.

2. Chemically polished copper showed etch pits (likely sulfer contaminants) with jagged edges.

3. Mechanically polished aluminum showed tears with jagged edges - perhaps caused also by soft impurities.

4. There were few emission sites seen on mechanically polished copper; no surface defects were found, and 50% of the microparticles that were found were seen to have sizes below 0.5 micron.

5. No dependence on oxide layers was seen for any cathode material; no difference was seen between OFHC and SE copper; and no enhancement was seen from grain boundaries - bare crystalline materials easily supported 200 MV/m.

6. Performance is dependent on preparation techniques, and most significantly on cleanliness.

Other Results

Cornell Group

- Results from superconducting rf cavities essentially the same as DC studies.

- Sensitive to surface defects that are not fully understood.

- Role of ion plasma in development of breakdown from field emission.

Kirby et al. (SLAC/IBM)

- Back to Fowler-Nordheim. Crystalline surfaces give good fits to theory.

Coatings (W.Peter et al, FMT Corp)

- Substantial reductions in field emission can be obtained, but these reductions are lost if breakdown occurs.

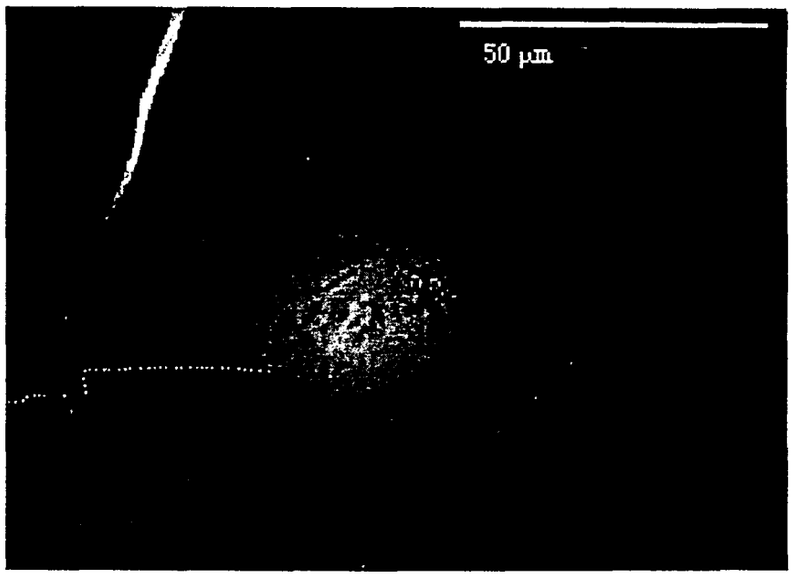

IGURE 9 Picture of a field emitter active at the end of the test. The micron sized craters at o'clock indicate the severity of the emission process. No foreign elements could be detected 'ith an EDX system at this site and no particulates were found.

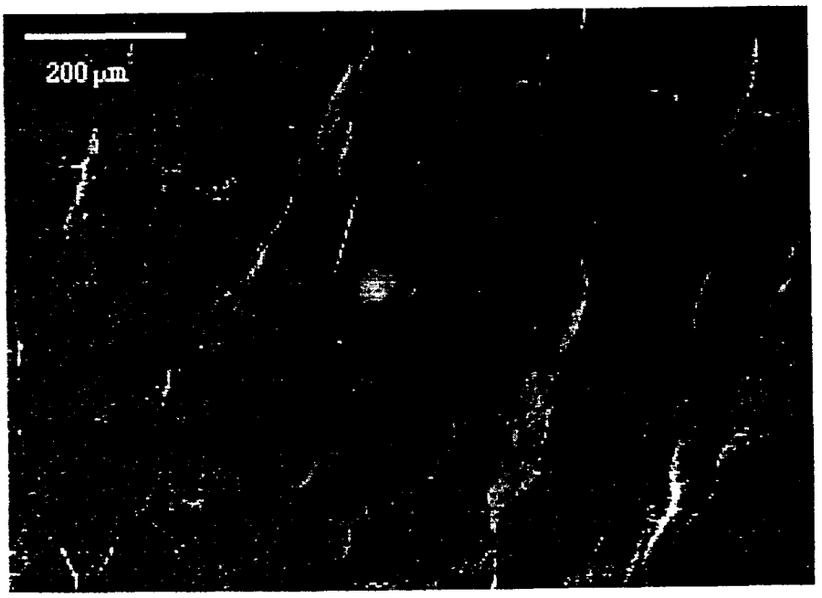

FIGURE 13 Low magnification photograph of the emitter in Figure **9** which was active at the end of the test. The starburst is indicative of plasma activity around the emitter despite the fact that the emitter did not process.

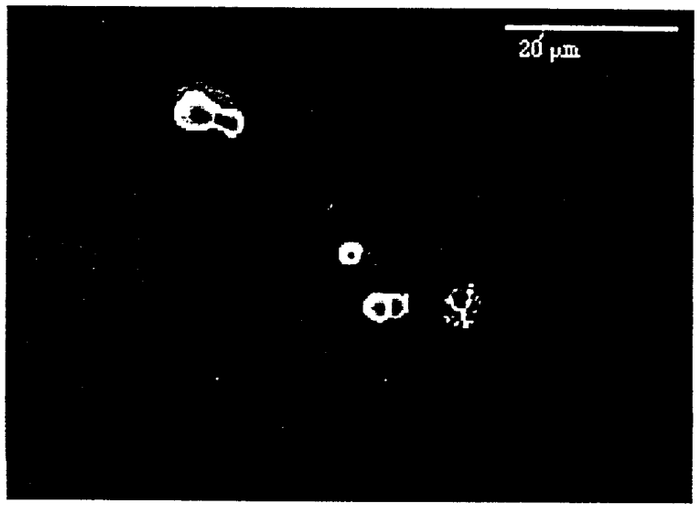

FIGURE 16 A field emitter found in a 5.8 GHz cavity. The previously molten iron particulate to the top left is too large to have been ejected by the craters and it is likely that it was melted by the same plasma that produced the starburst.

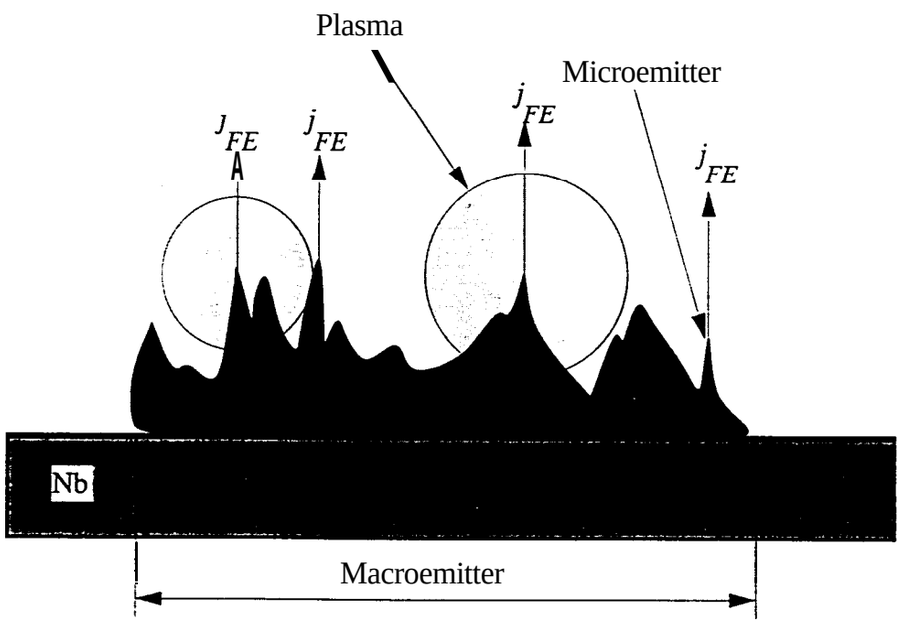

FIGURE 17 Schematic drawing illustrating a region of enhanced field emission (macroemitterj which is predominantly emitting from small areas within (microemitters). Due to the intense heating at the microemitters. neutrals are being desorbed and in turn are ionized by the emission current. It should be noted that, although in this figure the emission site is a particulate, this need not always be the case.

Ben-Yaacov, Back, and Kirby

Atomic Force Microscope (AFM)

Here it is!

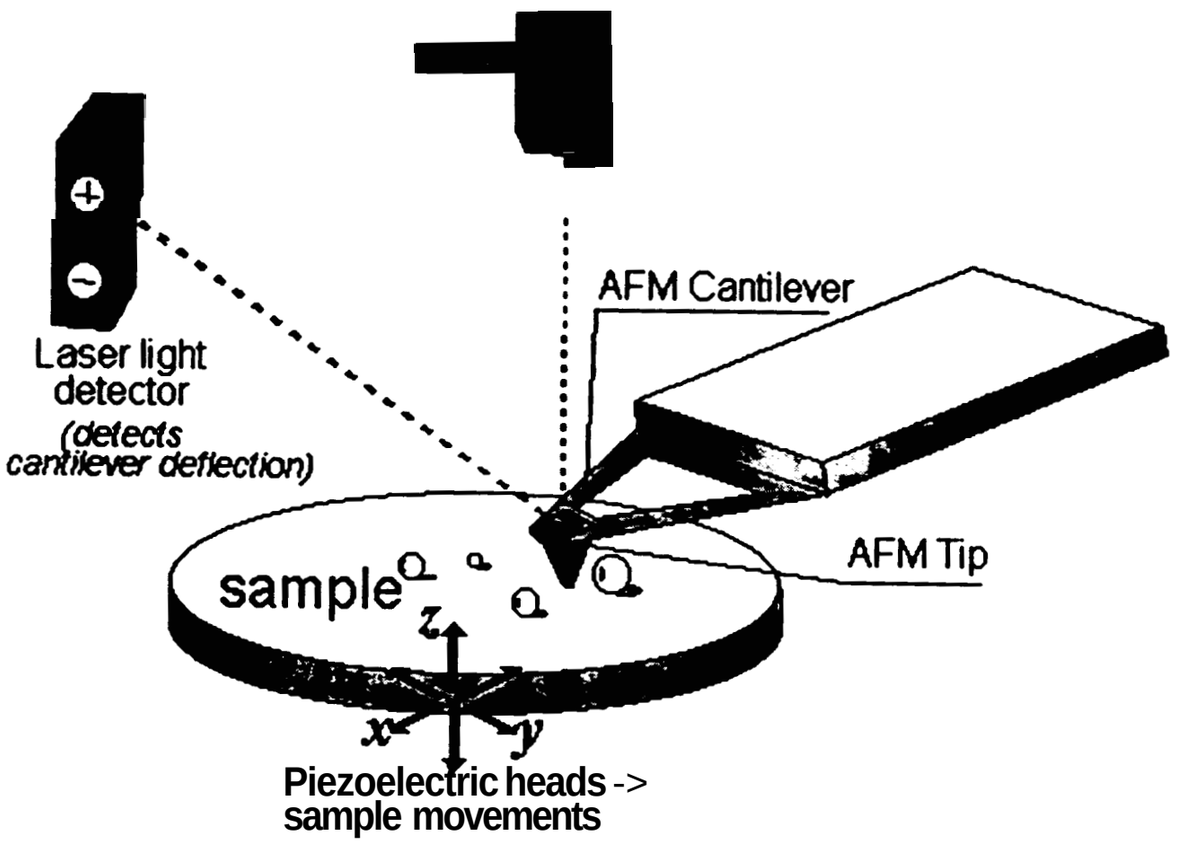

AWM

by

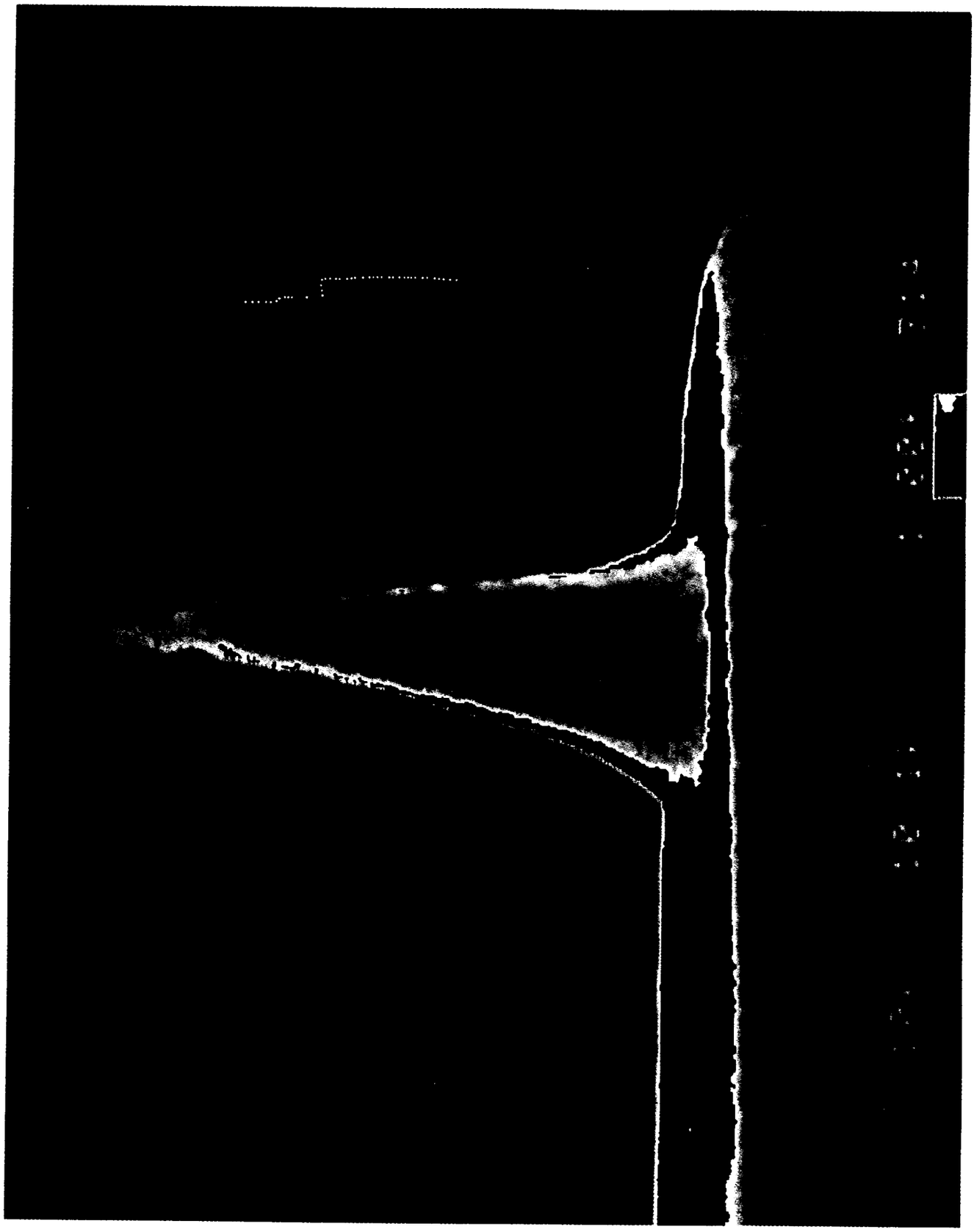

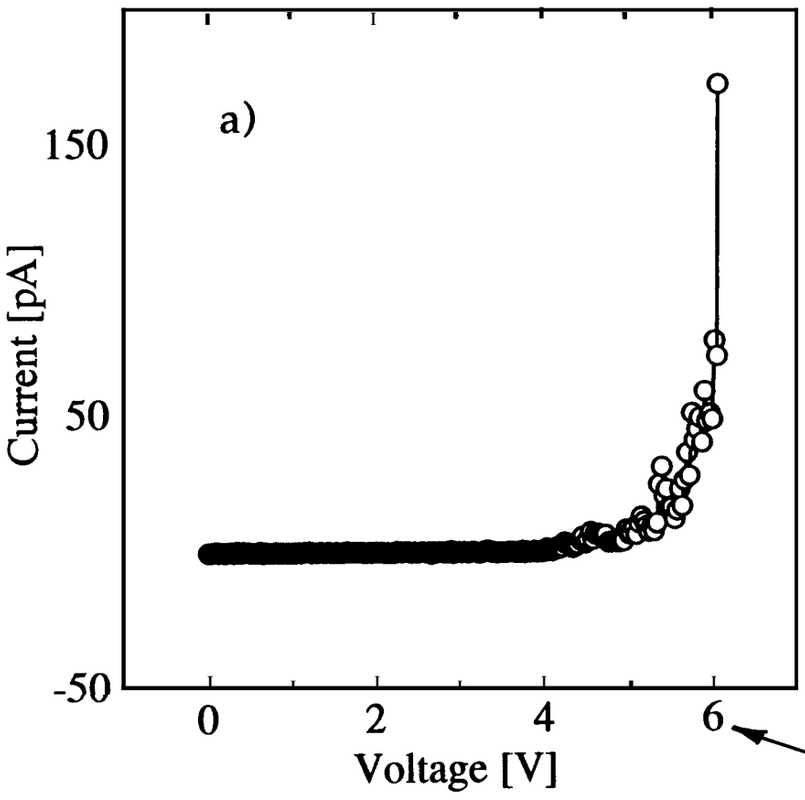

3-6 GV/m

Native oxide/OFE Cu

Typically 1-2 nm

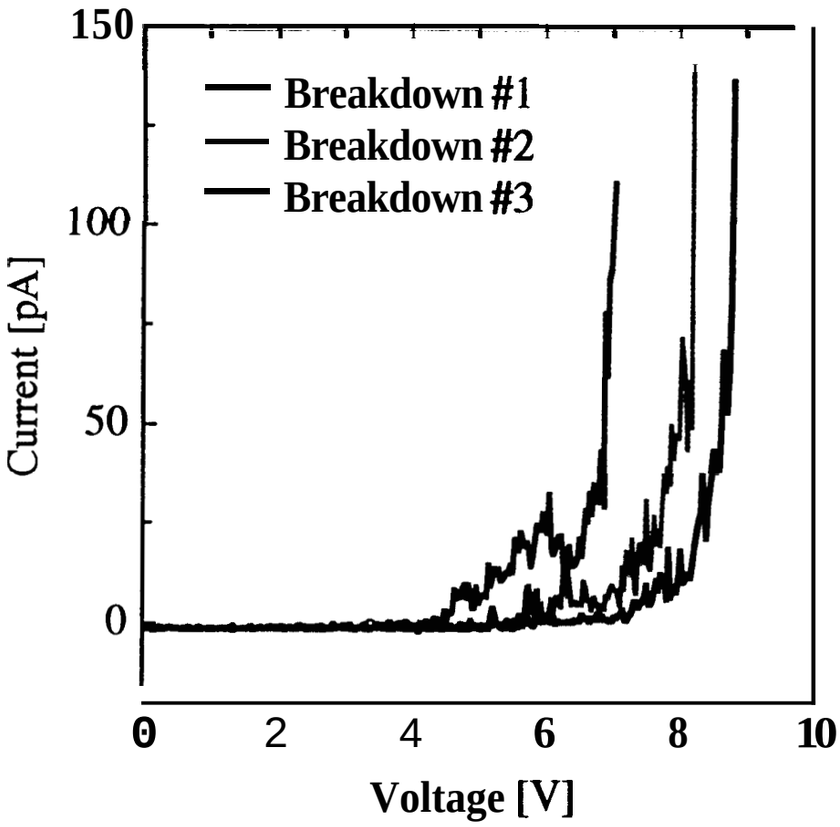

2.5 nm Al_2O_3/OFE Cu

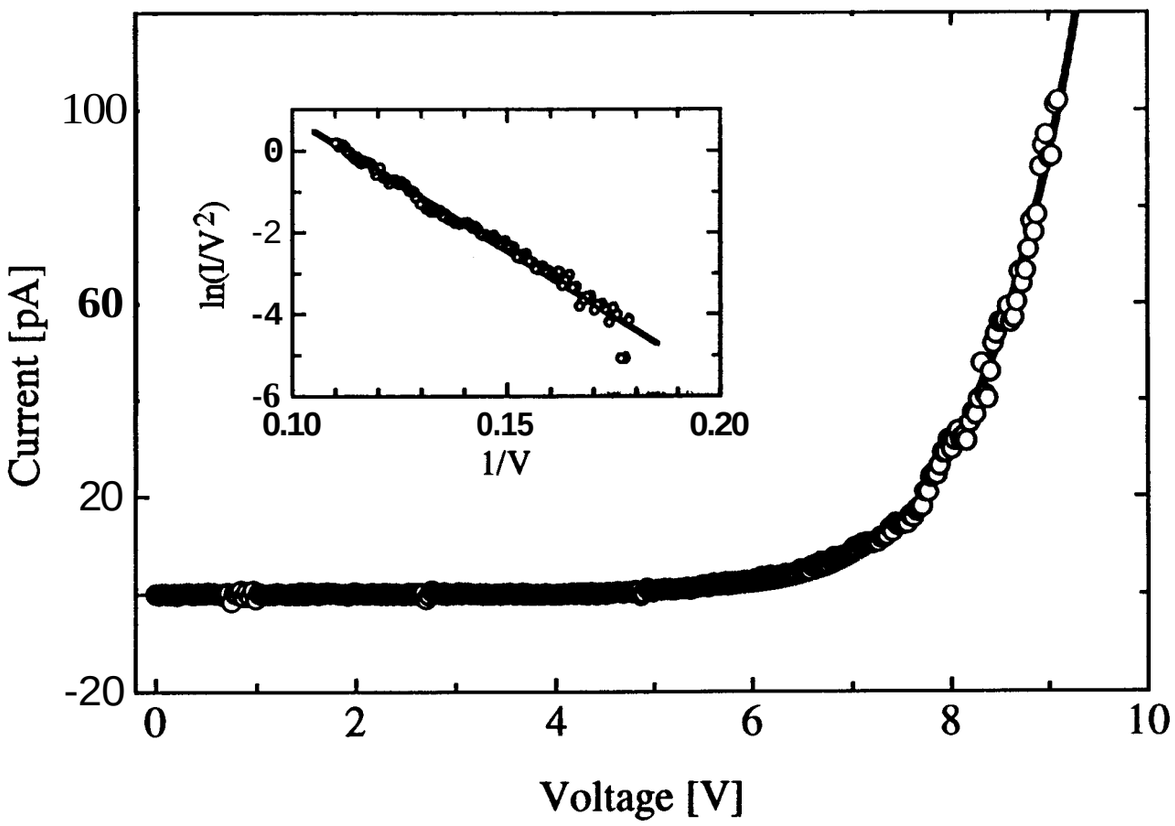

2.5 nm Al_2O_3 / 20 nm Pt / OFE Cu

Fit: $\phi = 4.5$ eV, $\beta = 1$

W. Peter, et al
FM Technologies Inc
1996

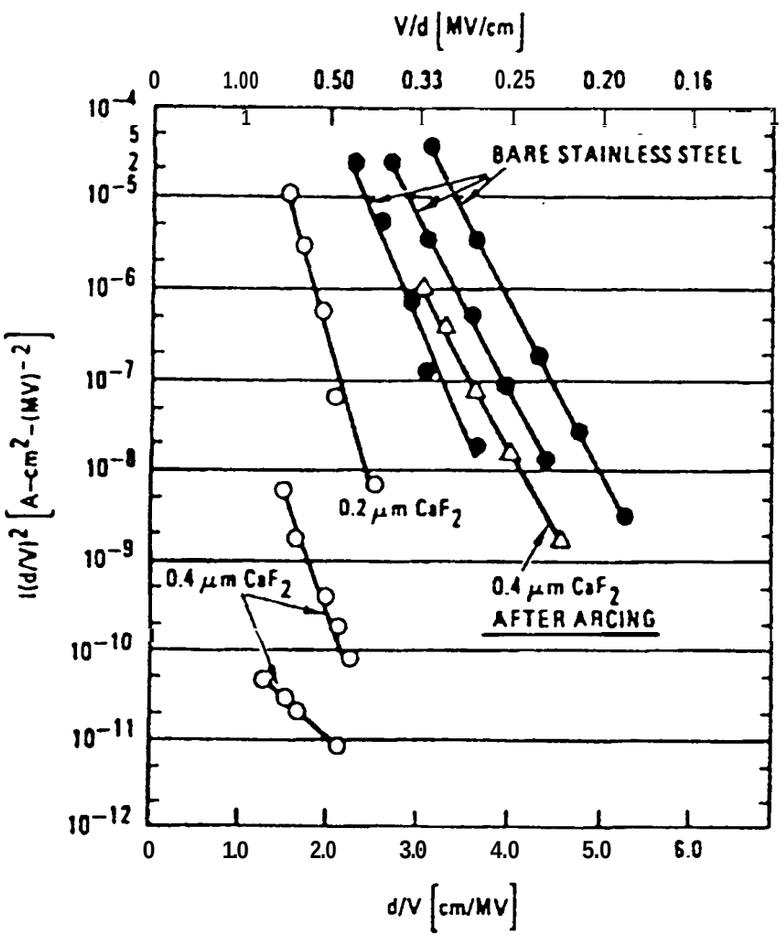

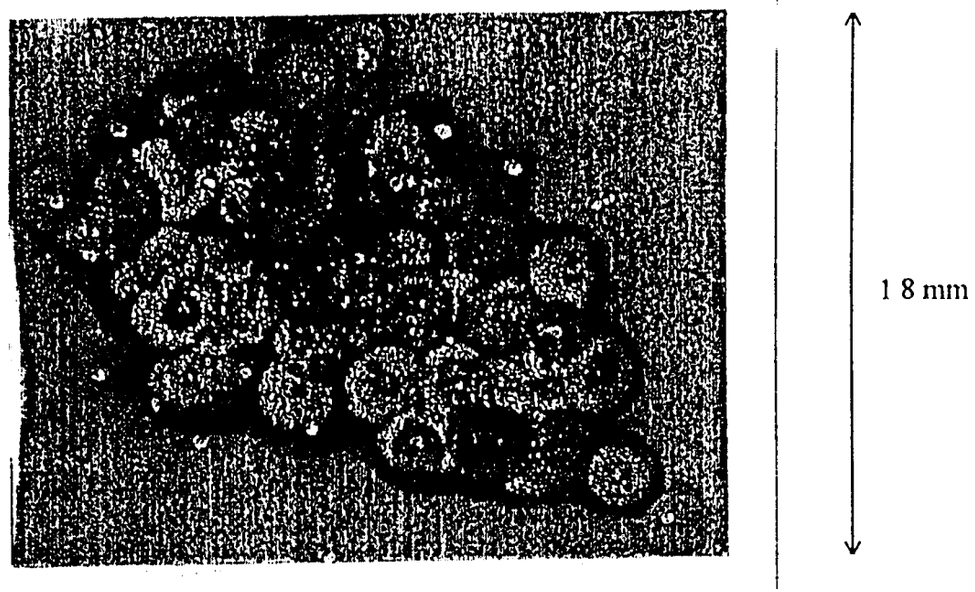

Snapshot of damage on he 5 μm CaF_2 disk at 50 times magnification. Coatings which had good voltage holdoff exhibited the most visible damage after breakdown due to the high voltage ai d the c pacitanoe of the coating, resulting in a high release of $CV^2/2$ energy.

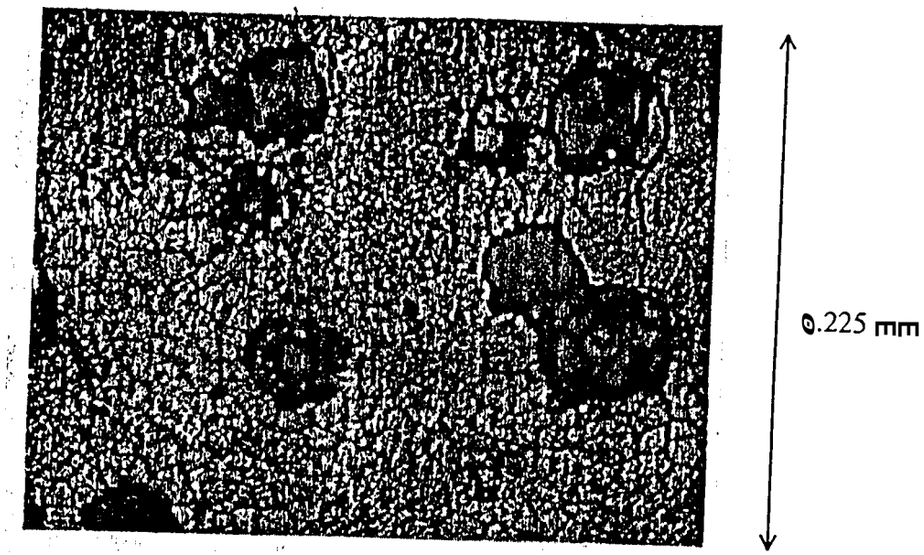

Snapshot of damage on the 5 μm CaF_2 disk at 400 times magnification. The damage is extensive and portions of the underlying Cu disk are now exposed.

Breakdown Voltages

FMT

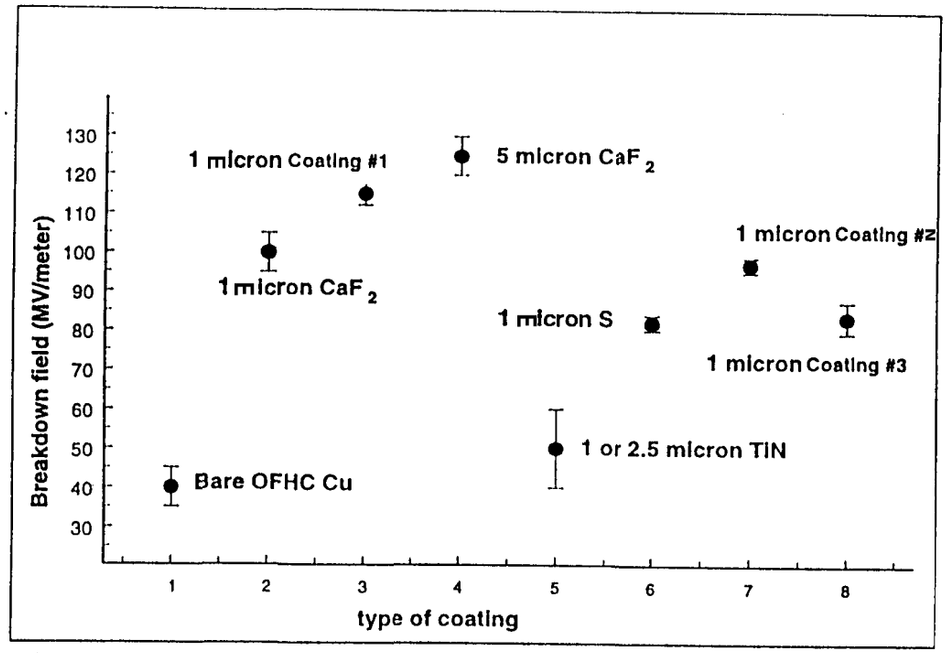

Summary of voltage breakdown values for different coatings on OHFC Copper.

Conclusions

- Field emission and breakdown originates from discrete sites that are sparsely distributed on crystalline surfaces.

- HV breakdown occurs at sites that field emit at lower voltages.

- Densities of potential emitters are small - typically $100/cm^2$ and usually less than $10^3/cm^2$.

- Potential emitters have dimensions of microns or less; these sites cover only a negligible fraction of the substrate surface, and only 5-10% of potential sites ever emit or breakdown.

- Potential emitters are predominately contaminants or surface defects introduced during manufacture and handling:

  e.g. Ag, Al, C, Ca, Cu, Cr, Fe, Mg, S, Si, Ti, W,
  etch pits in copper, tears in aluminum, scratches.

- Emitters generally (at least 80% of them and probably all) are conductors or semiconductors that have become attached to or embedded in the substrate; you have to **work** to get them to stay there!

- Fowler-Nordheim properly accounts for behaviour **of** pure crystalline substrates.

What's Important

- Careful sequencing of manufacturing steps, use of appropriate finishing and cleaning techniques, and maintenance of clean environments will likely lead to dramatic reductions of field emission and HV breakdown (processing time and damage).

- Special materials (such as *HIP* treated copper) are not expected to lead to substantial improvements, and use of coatings should be avoided (or at best, limited to **only** special applications).

Thermal Properties of Breakdown

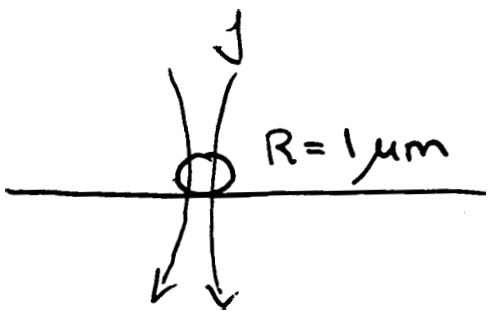

$$\Delta E = C \cdot \Delta T \cdot \text{mass}$$

	C	T_{melt}	d	**P**
Cu	.385	1085	8.9	1.54
Fe	.449	1538	7.9	8.51
	$\frac{J}{g\,^{\circ}K}$	°C	$g_m/_{cm^3}$	Ω·m

eg. Fe $\quad \Delta E_{melt} = 0.4\left(\frac{J}{g\,^{\circ}K}\right) \cdot 1.5\times10^{3}\,^{\circ}K \cdot (4\times10^{-11}\,g)$

$= 25\,nJ$

Cu $\longrightarrow$ 15 nJ

Current needed to melt sphere during rf pulse?

$$\frac{\Delta T}{\Delta t} = \frac{1}{C}\,\frac{\Delta E}{gm} = \frac{j^2 \cdot \rho}{C \cdot \text{density}}$$

$$= \frac{500^\circ K}{n\,sec}\left[\frac{j\ (A/m^2)}{10^{13}\ (A/m^2)}\right]^2$$

$\Delta t = 1$ ns (rf cycle) $\rightarrow$ $j = 1.5 \times 10^{13}$ A/m^2

$= 100$ns (rf pulse) $\rightarrow$ $j = 10^{12}$ A/m^2

Total Energy Needed to Spark?

Circuit model:

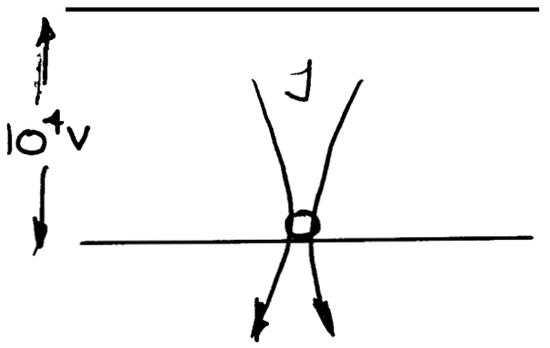

$$I_{TOT} = j \cdot \text{area} = 10^{13}\ A/m^2 \cdot 3\times10^{-12}\ m^2$$

$$= 30\ A$$

$$\Delta E_{TOT} = P\,\Delta t = IV\,\Delta t$$

$$= 3\times10^{5}\ J/sec \cdot 100\ nsec$$

$$= 30\ mJ$$

e.g. Resonant Ring : 100 mJ
Klystron Pulse : 40 J